Article

Hormetic Promotion of Biofilm Growth by Polyvalent Bacteriophages at Low Concentrations

Bo Zhang,[‖] Pingfeng Yu,*,[‖] Zijian Wang, and Pedro J. J. Alvarez*

Cite This: *Environ. Sci. Technol.* 2020, 54, 12358−12365

Read Online

ACCESS | 📊 Metrics & More | 📖 Article Recommendations | 🆂�🅸 Supporting Information

ABSTRACT: Interactions between bacteriophages (phages) and biofilms are poorly understood despite their broad ecological and water quality implications. Here, we report that biofilm exposure to lytic polyvalent phages at low concentrations (i.e., 10^2-10^4 phages/mL) can counterintuitively promote biofilm growth and densification (corroborated by confocal laser scanning microscopy (CLSM)). Such exposure hormetically upregulated quorum sensing genes (by 4.1- to 24.9-fold), polysaccharide production genes (by 3.7- to 9.3-fold), and curli synthesis genes (by 4.5- to 6.5-fold) in the biofilm-dwelling bacterial hosts (i.e., *Escherichia coli* and *Pseudomonas aeruginosa*) relative to unexposed controls. Accordingly, the biofilm matrix increased its polysaccharide and extracellular DNA content relative to unexposed controls (by 41.8 ± 2.3 and 81.4 ± 2.2%, respectively), which decreased biofilm permeability and increased structural integrity. This contributed to enhanced resistance to disinfection with chlorine (bacteria half-lives were 6.08 ± 0.05 vs 3.91 ± 0.03 min for unexposed controls) and to subsequent phage infection (biomass removal was 18.2 ± 1.2 vs 32.3 ± 1.2% for unexposed controls), apparently by mitigating diffusion of these antibacterial agents through the biofilm. Overall, low concentrations of phages reaching a biofilm may result in unintended biofilm stimulation, which might accelerate biofouling, biocorrosion, or other biofilm-related water quality problems.
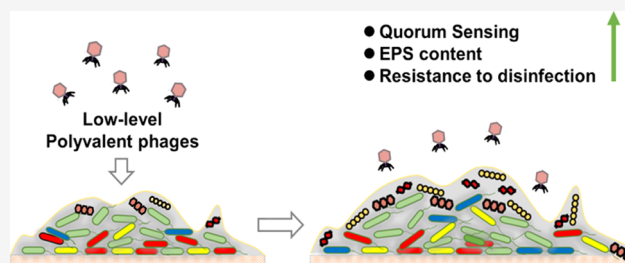
INTRODUCTION

Biofilms, which are attached and aggregated microbes surrounded by an extracellular polymeric substance (EPS) matrix,[1] are widespread in natural ecosystems and are increasingly utilized in wastewater treatment due to their resistance to exogenous stresses.[2,3] However, biofilms can also shelter pathogenic and other problematic microorganisms.[4−6] Considering their ecological significance and broad impacts,[7,8] there is a critical need to advance understanding of factors that shape biofilm structure and function.[9] This includes the influence of phages (i.e., bacterial viruses that constitute the most abundant and diverse biological entities in the biosphere),[10] which may modify biofilms through bacterial predation and horizontal gene transfer.[11]

Numerous experimental and computational studies have investigated biofilm−phage interactions in natural, engineered, and human environments.[12−14] The structural and functional stability of biofilms in the presence of phages generally benefits from the spatial heterogeneity of the biofilm matrix[15] and the diversity of dwelling bacteria.[7] Phages with broad host range and coding for EPS-degrading enzymes have fitness advantages within biofilms and may exhibit high efficiency for biofilm eradication.[16,17] However, the initial phage concentration can significantly influence both phage mobility and bacteria−phage coexistence in biofilms.[18,12] Whereas higher phage concentrations can accelerate biofilm removal and enhance phage mobility,[19] low phage concentrations may allow more response

time for bacterial adaptation and facilitate bacteria−phage coexistence within the biofilm.[20]

Physical stressors (e.g., UV radiation) and chemical stressors (e.g., antibiotics and disinfectants) at sublethal levels may stimulate biofilm formation,[21,22] which would enhance biofilm resistance and protect the bacteria within from antimicrobial agents. These responses could be related to hormesis, which is a biphasic dose response, in which the presence of low doses of toxicants can activate general repair mechanisms such as the error-free DNA repair processes that enhance resource allocation efficiency and overcompensate for toxic exposure.[23,24] In certain microenvironments (including water storage and distribution systems), the concentration of phages that reach biofilms could significantly decrease due to dilution, off-target attachment, and natural decay.[25−27] However, it is unknown whether low phage concentrations may similarly trigger biofilm stimulation. In theory, biofilm-dwelling bacteria could respond to phages with higher EPS secretion to limit

phage mobility,[13] following the same strategy to mitigate the impact of chemical antibacterial agents.

Given the increasing interest in using phages as supplements and alternatives for chemical-free eradication of problematic biofilms,[18,28,29] care should be taken of unintended counterproductive biofilm stimulation at low doses. Furthermore, advancing understanding of how phages shape biofilm structure and resistance may inform efforts to improve the efficacy of biofilm-based wastewater treatment processes or mitigate problems associated with undesirable biofilm formation (e.g., biofouling and microbial-induced corrosion). Therefore, it is important to elucidate how biofilms respond to different phages at various concentrations.

In this study, we investigate the dose–response behavior of dual-species biofilm systems (i.e., *Escherichia coli* and *Pseudomonas aeruginosa*) to two different phages. Particularly, we assessed the changes in attached biomass, bacterial viability, and phage abundance after treatment with different concentrations of polyvalent phages PEB1 and PEB2, respectively. EPS including polysaccharides, proteins, and eDNA were measured and visualized to corroborate the enhanced biofilm growth under low dose of polyvalent phages. We also analyzed the transcriptional expressions of biofilm-related genes (i.e., quorum sensing production, EPS excretion, and bacterial curli formation) under exposure to relatively high or low doses of polyvalent phages. This is the first demonstration that the exposure of biofilm to low dosage of polyvalent phages can upregulate quorum sensing genes and stimulate bacterial EPS production, which enhanced biofilm resistance to multiple stressors.

■ MATERIALS AND METHODS

Bacteria, Phage, and Culture Conditions. The bacterial strains in this study include *E. coli* K-12 (ATCC 10798) and *P. aeruginosa* PAO1 (ATCC 15692). *E. coli* represents an enteric pathogenic bacterium,[30] and *P. aeruginosa* is an opportunistic pathogen commonly active in biofilm formation.[31] These bacterial strains were routinely grown in the tryptic soy broth (TSB) medium at 37 °C while shaking overnight and then transferred to the modified M63 medium for dual species biofilm growth. Phages in this study include two polyvalent phages PEB1 and PEB2[19] (see Table S1 for growth parameters), which were selected by virtue of their capacity to infect both dominant species in our biofilm, *E. coli* and *P. aeruginosa*, to assess species-specific transcriptomic (hormetic) response variability. Total viable bacteria were counted by a plate assay using standard bacterial count agar (BD, Sparks, MD) and expressed as colony-forming units (CFU). *E. coli* was enumerated on eosin methylene blue (EMB) selective agar (CRITERION, Santa Maria, CA). *P. aeruginosa* was enumerated on Difco *Pseudomonas* selective agar (BD, Sparks, MD). Phages were enumerated using the double-layer plaque assay and expressed as plaque-forming units (PFU).[32]

Biofilm Formation and Phage Treatments. Ten microliters of *E. coli* and 10 μL of *P. aeruginosa* (with an initial optical density of 0.1 at 600 nm for each strain) were inoculated in 180 μL of modified M63 medium (i.e., 2.4 g of KH_2PO_4, 5.6 g of K_2HPO_4, 1.6 g of $(NH_4)_2SO_4$, and 0.3 mg of $FeSO_4$ per liter water supplemented with 1 mM $MgSO_4$, 0.2% glucose, and 0.5% casamino acids) in 96-well microtiter plates (REF 3879, Corning Incorporated). The microplates were incubated at 37 °C with horizontal shaking at 60 rpm for 48 h (the incubating medium was replaced with fresh medium every

12 h). Thereafter, the planktonic phase was removed and each well was washed twice with a phosphate buffered solution (PBS). Subsequently, 90 μL of SM buffer and 10 μL of phage were separately added to each well with final phage concentrations ranging from 10^2 to 10^8 PFU/mL. A control group (treated with 100 μL of SM buffer only) was also prepared to ensure that changes in biofilm were not caused by the SM buffer. After treatment for 6 h, different wells were used for characterization of different components (e.g., biofilm EPS, live bacteria, and phages). Each assay was conducted independently in triplicate.

For biofilm characterization, the wells were washed twice with PBS. The total attached biomass was quantified with a crystal violet optical assay as previously reported.[33] Briefly, 125 μL of 0.1% (w/v) crystal violet was added to the PBS-washed biofilm in each well and stained for 15 min in the dark at room temperature. Then, the excess dye was removed by washing twice with water. The attached crystal violet was destained with 125 μL of 30% acetic acid (v/v) solution, and the plate was read at a wavelength of 595 nm with a SpectraMax plus spectrometer (Molecular Device, Sunnyvale, CA). The experiments were performed in triplicate. The biofilm removal efficiency was calculated as the relative difference between the treated biofilm and control biofilm. To quantify the surviving bacteria and final phage counts, the treated biofilm was dispersed in PBS with Tween 20 by sonicating at 40 kHz for 5 min in a 4 °C bath sonicator (Branson, Danbury, CT).[17] Total viable bacteria were counted by the plate assay using standard bacterial count agar, and total phages were enumerated using the plaque assay plated on the *E. coli* lawn.[34]

Biofilm EPS Quantification. Biofilm EPS was characterized in terms of protein, polysaccharide, and extracellular DNA (eDNA) as previously reported.[35,36] Briefly, PBS-washed biofilms were dispersed in PBS with Tween 20 as described above. Samples from four wells with the same treatment were combined in 30 mL of 2% (w/v) EDTA (disodium salt) extracting solution, and the mixture was stirred at 4 °C for 3 h. The cells in each well were resuspended in one volume of deionized water, and then the suspension was centrifuged (4000 g for 5 min at 4 °C) to remove the bacteria.[37] The supernatants were then filtered through a 0.22-μm pore size filter. The protein content in the filtrate was measured with a BCA kit by UV/vis spectrophotometry using bovine serum as the standard (Sigma-Aldrich, St. Louis, MO), according to the kit manual. The total polysaccharide was analyzed according to the phenol–sulfuric acid colorimetric method using D-glucose as a standard.[38] The eDNA content was quantified with the diphenylamine reagent method using a calf thymus DNA as the standard.[39]

Biofilm Live/Dead Bacteria Analyses via CLSM. Confocal laser scanning microscopy (CLSM) was adopted to visualize the biofilm structure after phage treatment as previously reported.[19,33] Briefly, the residual biofilm in the 96-well plate was stained with SYTO 9 and propidium iodide (PI) from the LIVE/DEAD BacLight kit (Invitrogen, Basel, Switzerland). The biofilm sample was then loaded on the 96-well plate holder and observed using a 40× dry objective under the Nikon A1-Rsi CLSM (Nikon, Tokyo, Japan). The STYO 9-stained living bacteria emit green light when excited by a 488-nm laser line, and the PI-stained dead bacteria emit red light when excited by a 560-nm laser line.

Biofilm EPS Analyses via CLSM. The triple staining method was used for biofilm EPS (i.e., protein, polysaccharide,

and eDNA) analyses as follows. The biofilm was first stained with 20 mM SYTO 45 for eDNA visualization.[40] To protect amine groups, the biofilm was rinsed with 0.1 M NaHCO$_3$. Then, the protein was stained with 1 mg/mL fluorescein isothiocyanate (FITC) dissolved in dimethyl sulfoxide (DMSO).[41] Finally, α-D-glucopyranose in polysaccharides was stained with 200 mg/mL con-canavalin A-tetramethylr-hodamine (conA-tetramethylrhodamine).[42] Samples were washed twice with PBS after each dyeing step. The excitation laser wavelengths used for SYTO 45, FITC, and conA-tetramethylrhodamine were 455, 488, and 561 nm, respectively. The biofilm was scanned from top to bottom layers to investigate the biofilm responses to different phage dosages. Z-stack images were collected and rendered into three-dimensional (3D) images to visualize the structure of biofilm using Nikon NIS-Element software (Nikon, Tokyo, Japan).

Differential Gene Expression Analysis (RNA-seq and RT-qPCR). Biofilm samples were taken for transcriptomic analysis after phage treatment for 4 h, when both phage and bacteria abundance had stabilized after low-level phage exposure (Figure S1). Twelve genes regulating quorum sensing (QS) (*sdiA*, *luxS*, *lasI*, *lasR*), EPS generation (*pelA*, *pslA*, *rhlA*, *msbB*, *rcsF*), and curli biosynthesis (*csgB*, *csgD*, *sfaS*) were chosen for transcriptomic analysis (Table S2). The RNA polymerase C gene *rpoC*, which exhibits relatively stable expression levels in biofilm bacteria,[43] was used as a reference gene for gene expression normalization. Total RNA was extracted from biofilm samples using the RNeasy Mini Kit (Invitrogen, Thermo Fisher Scientific) and treated with Turbo DNAse at 5 U/mL for 30 min at 37 °C to remove residual DNA. Thereafter, the DNAse was heat-inactivated by incubation of samples at 65 °C for 10 min.[44] The quality of RNA was verified using a Nanodrop ND-1000 instrument (Nanodrop products Inc., Wilmington, NE). Subsequently, the reverse transcription-polymerase chain reaction (RT-PCR) analysis was conducted as previously described.[36] Briefly, 1 μg of purified RNA was converted into cDNA with iScript Reverse Transcription Supermix (Applied biosystem). Triplicate RT-qPCR reactions with 15 μL of reaction mixture (1 μL of cDNA template, 7.5 μL SYBR Green Master Mix, 0.5 μL for each primer, and 5.5 μL of water) were conducted using a Bio-Rad MyCycler thermal cycler (Bio-Rad Laboratories). The $2^{-\Delta\Delta CT}$ method was used to quantify differential gene expression relative to the reference gene, and the cycle threshold (CT) values used were the means of independent triplicates.[36] The heatmap showing the overall RT-qPCR array data of detected genes with relative abundance of detected genes for the relative gene abundances was performed in R platform (R version 3.2.2; www.rproject.org).

Infection of Pretreated Biofilms with Phages. Biofilms were pretreated with low-dose phage (L-biofilm, 10^4 PFU/mL), high-dose phage (H-biofilm, 10^8 PFU/mL), or no phage (C-biofilm) and then washed twice with PBS to remove the planktonic phase. Subsequently, 90 μL of SM buffer and 10 μL of phage solutions were added to each well to reach a phage concentration of 10^7 PFU/mL. After treatment 6 h, the total attached biomass was estimated using the crystal violet optical assay,[33] and biofilm removal efficiency was calculated as the relative difference between the biofilm and control biofilms. Two additional biofilm treatments were prepared using phages at two lower levels (i.e., 10^2 and 10^3 PFU/mL) to confirm the hormetic response.

Treatment of Pretreated Biofilms with Disinfectants. To investigate the effect of phages on biofilm resistance to disinfectants, some H-, L-, and C-biofilms were also treated with 10 ppm chlorine at room temperature. Different wells were used to quantify the total viable bacteria after treatment for 2, 4, 6, 10, 15, 20, and 30 min. The wells were washed twice with PBS, and the biofilms were dispersed in PBS with Tween 20, as described above. Total viable bacteria were counted by the plate assay. The biofilm bacteria decay after chlorine treatment was fitted with a first-order kinetics model (i.e., $C = C_0 e^{-kt}$), where k is the decay rate coefficient (min^{-1}), C_0 is the initial bacterial concentration (CFU/mL), and C is the bacterial concentration after chlorine treatment at t time (min). The bacterial half-life ($t_{1/2}$) was calculated as follows: $t_{1/2} = \ln 2/k$.

Statistical Analyses. All of the experiments were performed independently in at least triplicates. Analysis of variance (ANOVA) and Student's *t*-test with Bonferonni correction for multiple comparisons were used to determine statistical significance.

■ RESULTS AND DISCUSSION

Low Concentrations of Polyvalent Phages Promoted Biofilm Formation. Polyvalent phages may disperse through biofilms by infecting multiple bacteria species in the matrix.[45] The response of this biofilm (composed of 18 ± 1% *E. coli* and 82 ± 3% *P. aeruginosa* of the total cell counts) to polyvalent phages of different properties (Table S1) followed a hormetic trend, which is characterized by low-dose stimulation and high-dose inhibition.[46,47] Particularly, two polyvalent phages (PEB1 and PEB2) separately inhibited a dual species 48 h biofilm when initial phage concentrations ranged from 10^5 to 10^8 PFU/mL (with multiplicity of infection (MOI) from 10^{-4} to 10^{-1}, Figure 1). The biofilm biomass decreased significantly by 32.6 ± 2.5 and 39.0 ± 3.0% ($p < 0.05$) after treatment for 6 h with 10^8 PFU/mL PEB1 or PEB2, respectively. Phages PEB1
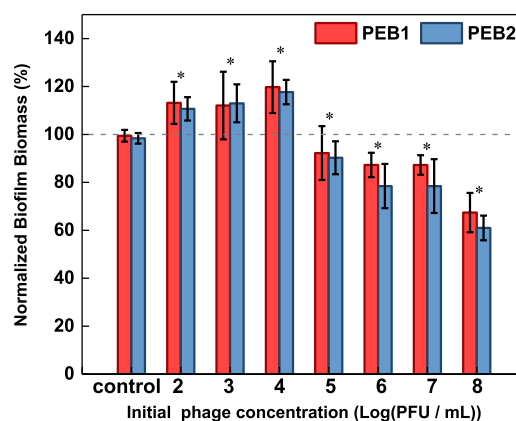
Figure 1. Biofilm biomass increased when exposed to low-dosage of polyvalent phages (PEB1 and PEB2). The two-species biofilm (i.e., *E. coli* and *P. aeruginosa*) was treated with different concentrations of phages at 37 °C for 6 h. Biomass was measured using the crystal violet stain assay. The biofilm biomass was normalized by the group before phage addition (dash line). Control represents the unexposed group (PFU = 0). Biofilms without phage infection were more stable than those that interacted with phages. Error bars represent ± one standard deviation from the mean of independent triplicates. Asterisks (*) represent significant differences ($p < 0.05$) between treatment and unexposed control, based on Student's *t*-test.

and PEB2 exhibited higher efficiency of infection toward *E. coli* relative to *P. aeruginosa* (Table S1). Accordingly, the final biofilm composition after phage treatment was similar to initial composition with *P. aeruginosa* continuing to dominate in the dual-species biofilms (Figure S2). Due to bacterial lysis and phage propagation, PEB1 and PEB2 titers increased to 4.5-log and 3.6-log, respectively, after treatment (Figure 2). Surpris-
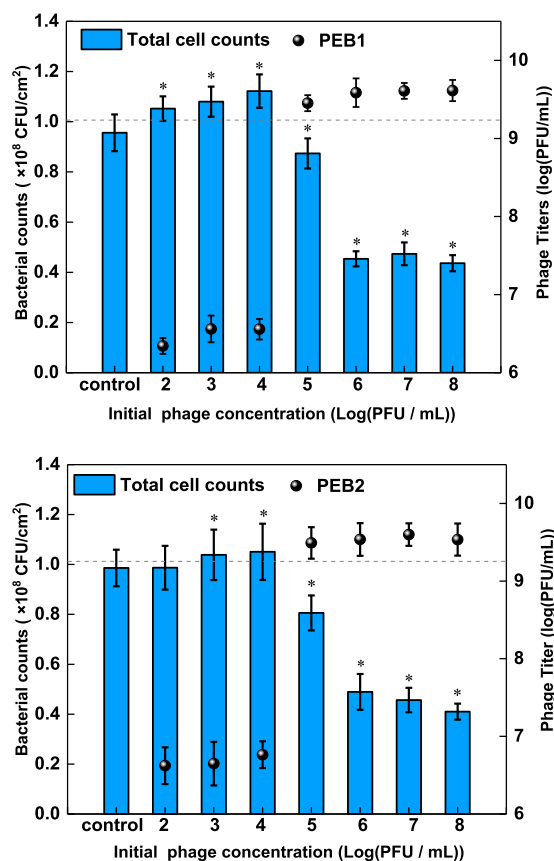
Figure 2. Total cell counts and phage titer after exposure of 6 h to phages PEB1 and PEB2. *E. coli* and *P. aeruginosa* were enumerated with the plate assay using *E. coli* and *Pseudomonas* selective agars, respectively. The total cell counts were calculated as the sum of *E. coli* and *P. aeruginosa*. The total cell counts were normalized by the cell counts in the group before phage addition (dash line). The absolute numbers of *E. coli* and *P. aeruginosa* are shown in Table S3. Asterisks (*) represent significant differences ($p < 0.05$) between treatment and unexposed control, based on Student's *t*-test.

ingly, when the initial phage concentrations ranged from 10^2–10^4 PFU/mL (with MOI from 10^{-7} to 10^{-5}), PEB1 and PEB2 exerted a clear stimulatory effect on the biofilm. The maximum biomass increase ($19.7 \pm 2.2\%$ with PEB1 and $17.8 \pm 2.0\%$ with PEB2) was obtained when the biofilm was exposed to 10^4 PFU/mL phages. Note that the dual species biofilm experienced marginal growth when no phages were introduced (Figure 1). A similar stimulation pattern was observed with a 72 h biofilm exposed to a low concentration of these phages (Figure S3).

Similar hormetic responses of biofilms have been previously observed in response to physical and chemical stressors[48,49] but not in response to phages. Apparently, this is an adaptive response (e.g., overcompensation stimulation and receptor-mediated stimulation)[48,50] to optimize bacterial survival through increased biofilm spatial heterogeneity and hindered

diffusion of antibacterial agents. For example, the physical barrier conferred by the growing biofilm matrix can hinder phage infection and propagation in biofilms.
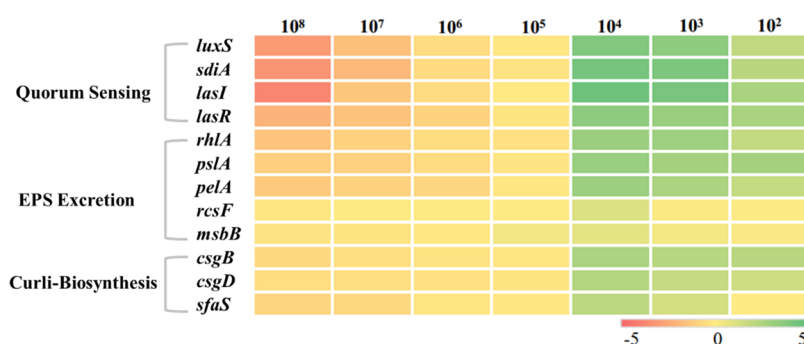
Low Concentrations of Polyvalent Phages Upregulated QS Generation, EPS Excretion, and Curli Biosynthesis Genes. Bacterial QS systems can mediate bacterial intraspecies and interspecies communication through signal molecules (e.g., autoinducers) and regulate their behavior such as biofilm formation to adapt environmental changes.[51,52] The transcriptomic analysis suggests that biofilm stimulation by phages at low concentrations involves the QS systems of both bacterial species. Four genes regulating QS secretion (i.e., *sdiA* and *luxS* in the *lux* QS system of *E. coli*, *lasI* and *lasR* in the *las* QS system of *P. aeruginosa*) were upregulated by 4.1 to 24.9-fold upon exposure to low phage levels (i.e., 10^2–10^4 PFU/mL) relative to control groups without phage exposure (Figure 3). For example, *rhlA* in *P. aeruginosa* (regulated by the *las* QS system to participate in rhamnolipid transferase synthesis) was overexpressed by up to 9.3-fold. Polysaccharide-related genes (*pslA* and *pelA*) were also upregulated (by at least 3.7-fold) upon exposure to low phage concentrations (Figure 3). In contrast, these genes were slightly suppressed upon exposure to high phage levels (i.e., 10^5 to 10^8 PFU/mL).

Whereas significant upregulation of genes associated with polysaccharide synthesis (e.g., colanic acid and lipopolysaccharide) was not detected in *E. coli*, genes encoding biosynthesis of curli substances experienced a higher expression level after exposure to low dosage of phages. Genes *csgB* (involved in curli production) and *csgD* (associated with curli transcription and transport) increased by 6.5- and 5.3-fold, respectively, relative to unexposed controls. Enhanced expressions of *sfaS*, which encodes S-fimbrial adhesins in *E. coli*, were also observed (by up to 4.5-fold) after exposure to phages at low concentration.[53]

Overall, upregulation of these detected genes is conducive to biofilm formation and maturation, resulting in a denser biofilm (Figures S4 and S5) with enhanced resistance to phage penetration during subsequent infections. Accordingly, phage propagation was significantly inhibited by previous exposure and acclimation to low phage concentration (Figure 2), as reflected by a marginal decrease in biofilm bacteria concentration (1.06 ± 0.04 vs $1.05 \pm 0.03 \times 10^8$ CFU/cm^2) and a little increase in phage titer (4.8 ± 0.2 vs $5.0 \pm 0.4 \times 10^6$ PFU/mL) between exposure of 4 and 6 h (Figure S1).

Low Concentrations of Polyvalent Phages Increased Biofilm Matrix Components. Biofilm EPS components (i.e., proteins, polysaccharides, and eDNA) were quantified to corroborate the transcriptional results after exposure to the low level of phages. Consistent with changes in biomass, the biofilm EPS content decreased significantly after treatment with high concentration of polyvalent phages (10^5–10^8 PFU/mL) and increased after exposure to low phage concentrations (10^2–10^4 PFU/mL) (Figure 4). Stimulation of extracellular polysaccharide and eDNA production contributed the most to EPS formation. Particularly, the biofilm extracellular polysaccharide and eDNA increased by 41.8 ± 2.3 and $81.4 \pm 2.2\%$, respectively, after exposure to 10^4 PFU/mL PEB1, and by 43.7 ± 1.8 and $95.5 \pm 2.0\%$ after exposure to the same concentration of PEB2.

CLSM images also show that both polysaccharides and eDNA content increased significantly after low-level phage treatment, while all of the EPS components decreased dramatically following treatment with high phage concen-

Figure 3. Upregulation of quorum sensing, EPS excretion, and curli biosynthesis genes following exposure to low concentrations of polyvalent phages. RT-qPCR was performed targeting the QS generation, EPS excretion, and curli biosynthesis-related genes. The quantification of each gene was expressed as the fold change (fold changes are log 2 transformed) relative to unexposed controls. The top X-axis is the initial phage concentration (PFU/mL) in the bulk solution. Results are the mean of independent triplicates.
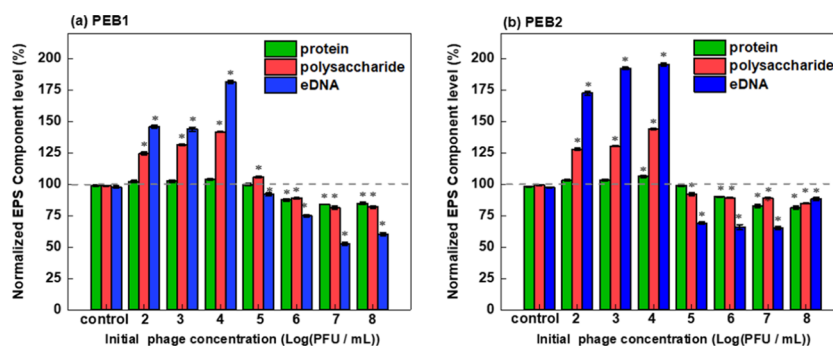
Figure 4. Changes in biofilm EPS content after phage treatment. (a) Normalized EPS component (protein, polysaccharide, and eDNA) level after treating with phage PEB1; (b) Normalized EPS component (protein, polysaccharide, and eDNA) level after treating with phage PEB2. The protein content was measured by UV/vis spectrophotomety using a BCA kit. The total polysaccharide content was analyzed using the phenol−sulfuric acid colorimetric method, and the eDNA content was quantified with the diphenylamine reagent method. These components were normalized by those in the group before phage addition (dash lines). Asterisks (*) represent significant differences ($p < 0.05$) between treatment and unexposed control, based on Student's t-test. Error bars represent $\pm$ one standard deviation from the mean of six independent replicates.

trations (Figure 5). The biofilm thickness varied slightly after low-level phage exposure, while it became much denser with higher levels of EPS (0.88 ± 0.02 vs 0.70 ± 0.02 volumetric fraction as determined by CLSM software) and more compact bacteria (0.75 ± 0.01 vs 0.62 ± 0.02 volumetric fraction) relative to unexposed controls (Figures S4 and S5). Furthermore, the final biofilm biomass was positively correlated with the total biofilm EPS contents ($p = 0.007$) instead of the pattern in viable cell numbers ($p = 0.156$), indicating that the observed increase in biofilm biomass was primarily due to EPS production rather than cell growth. Furthermore, the changes in eDNA and polysaccharide components accounted for 47.6% ($p = 0.0150$) and 33.3% ($p = 0.0471$) variation of biofilm biomass, respectively. Previous studies have demonstrated that higher EPS content enhances the mechanical stability of biofilms,[54] which contributes to resistance to various stresses.

The EPS matrix increases biofilm spatial heterogenicity and serves as a physical barrier to protect bacteria from multiple environmental stressors including phage infection.[1,55] Enhanced EPS matrix production at low phage concentrations can hinder phage diffusion into biofilm through phage adsorption and size exclusion, which may disrupt phage attachment onto their bacterial hosts (the first step of phage infection) and inhibit phage offspring dissemination after successful infection.[56] Particularly, polysaccharides with high viscosity can directly adsorb phages and increase cross-linking

within the biofilm by interacting with themselves or other heterologous molecules.[57] Moreover, eDNA can function as an intercellular connector through hydrogen bonding and electrostatic interactions,[58] which helps maintain biofilm structural integrity.[59]

Enhanced Biofilm Resistance to Both Chemical Disinfectants and Subsequent Phage Infection after Stimulatory Exposure to Low Concentrations of Polyvalent Phages. The biofilm pre-exposed to a low concentration of polyvalent phages (L-biofilm, pretreated with 10^4 PFU/mL) showed enhanced resistance toward subsequent infection by high phage concentrations relative to the control biofilm without prior phage exposure (C-biofilm) and the biofilm pre-exposed to high concentration of polyvalent phages (H-biofilm, pretreated with 10^8 PFU/mL) (Figure 6). Particularly, the biomass removal efficiency of L-biofilm, C-biofilm, and H-biofilm by subsequent exposure to 10^7 PFU/mL phage PEB1 was 17.1 ± 2.2, 31.6 ± 1.7, and 41.5 ± 2.3%, respectively. Similarly, the biomass removal efficiency of L-biofilm, C-biofilm, and H-biofilm by 10^7 PFU/mL phage PEB2 was 19.2 ± 3.0, 32.9 ± 2.7, and 39.5 ± 2.5%, respectively. Similar patterns of enhanced resistance were also observed in biofilms pretreated with phages at other low exposure levels (i.e., 10^3 and 10^2 PFU/mL) (Figure S6).

L-biofilms treated with PEB1 and PEB2 separately were also more tolerant to the chemical disinfectant, chlorine, compared to the C- and H-biofilms (Figure S7). Biofilm bacteria decay
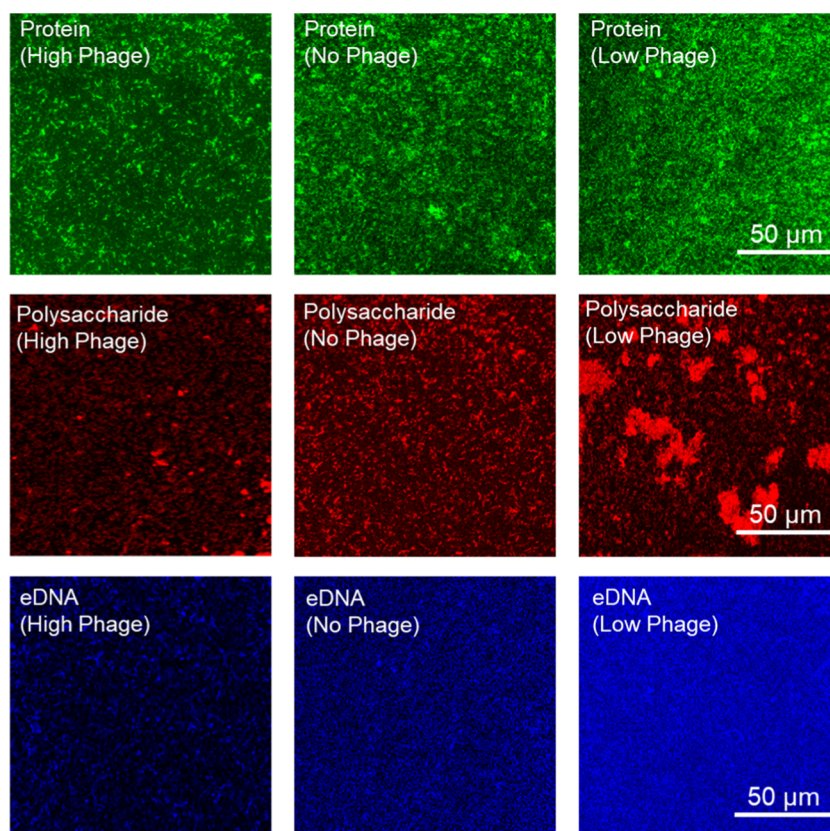
Figure 5. Confocal laser scanning microscopy images show a pronounced increase in protein, polysaccharides, and eDNA content in the EPS of biofilm exposed to a low concentration of phages. The biofilm was first stained with 20 mM SYTO 45 for eDNA visualization. Then, the protein was stained with 1 mg′/mL fluorescein isothiocyanate (FITC) dissolved in DMSO, and the polysaccharides were stained with 200 mg/mL con-canavalin A-tetramethylrhodamine (conA-tetramethylrhodamine). High phage exposure was 10^8 PFU/mL, and low phage exposure was 10^4 PFU/mL. The green, red, and blue color intensity represents the abundance of EPS proteins, polysaccharides, and eDNA, respectively.
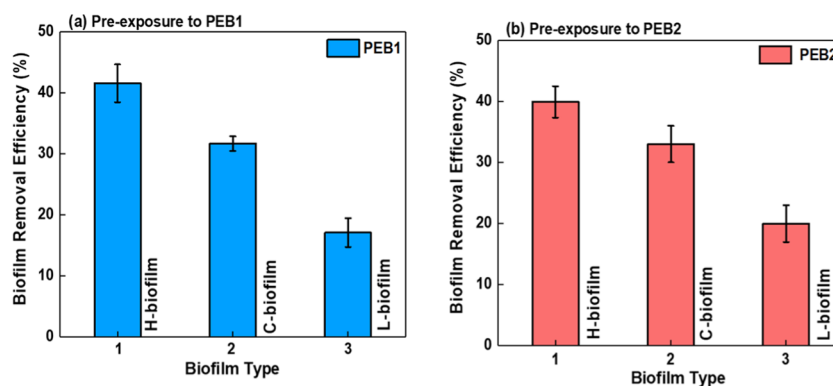
Figure 6. Biofilm pretreated with a low concentration of phage ((a) PEB1 and (b) PEB2) displayed enhanced resistance toward a second infection with high phage concentration. H-biofilm, C-biofilm, and L-biofilm represent the biofilm pretreated with phages at three levels (10^8, 0, and 10^4 PFU/mL), respectively. These pretreated biofilms were then infected again with high levels of phage (10^7 PFU/mL) for another 6 h. Error bars represent ± one standard deviation from the mean of independent triplicates.

followed first-order kinetics with half-lives of 6.08 ± 0.05, 3.91 ± 0.03, and 3.35 ± 0.03 min for PEB1-pretreated L-, C-, and H-biofilms, respectively. Bacteria decay in PEB2-pretreated biofilm followed similar trends with half-lives of 5.95 ± 0.05, 3.98 ± 0.04, and 3.58 ± 0.03 min for L-, C-, and H-biofilms, respectively. Apparently, the more abundant and denser gel-like EPS matrix (the total EPS volume increased by 25.7 ± 0.9% and EPS mass content increased by 31.9 ± 2.7% compared to the control ones) limited the diffusion of phages and chemical disinfectants through the biofilm and protected the deeper layers of cells from subsequent phage infection or chemical damage.[49,55]

We recognize that different polyvalent phages may exhibit different host preferences and proliferation thresholds[32,60] and thus some phages may exert dissimilar pressures and elicit different extents of differentiation and biofilm stimulation for different bacteria. Nevertheless, we observed a consistent pattern (e.g., stimulated biofilm formation and densification through hormetic upregulation of quorum sensing, EPS production and curli genes) for two phages with different

properties and two different bacterial genera. Accordingly, we postulate that (similar to the response of biofilms to physical and chemical stressors)[21,22] this was a hormetic response—particularly, a stimulatory response to the presence of low doses of a stressor that triggered a general repair or defense mechanisms[23] to overcompensate for that stress.

Overall, biofilms are known to deteriorate treatment process performance (e.g., membrane biofouling), harbor pathogens, and accelerate water infrastructure corrosion. Due to phage dilution, off-target adsorption, or natural decay, biofilm can be transiently exposed to low-level phages, which may subsequently promote biofilm growth and enhance biofilm resistance to antimicrobials. This implies that low-level phage exposure might be an overlooked contributor to biofilm-relevant problems in water systems and highlights the need for systematic investigations of dose–response relationships between different types of biofilms and phages to avoid unintended consequences.

■ ASSOCIATED CONTENT

Supporting Information

The Supporting Information is available free of charge at https://pubs.acs.org/doi/10.1021/acs.est.0c03558.

> Bacterial composition in initial and treated biofilms; biofilm of different maturity in response to phages; biofilm resistance to reinfection by high phage concentration; biofilm bacteria decay rate during disinfection with chlorine; phage growth parameters in different hosts; detailed information on functional genes (PDF)

■ AUTHOR INFORMATION

Corresponding Authors

Pingfeng Yu − Department of Civil and Environmental Engineering, Rice University, Houston 77005, United States; Email: pingfeng.yu@rice.edu

Pedro J. J. Alvarez − Department of Civil and Environmental Engineering, Rice University, Houston 77005, United States; orcid.org/0000-0002-6725-7199; Email: alvarez@rice.edu

Authors

Bo Zhang − School of Environment, Harbin Institute of Technology, Harbin 150090, China

Zijian Wang − School of Civil and Environmental Engineering, Cornell University, Ithaca, New York 14853, United States

Complete contact information is available at:
https://pubs.acs.org/10.1021/acs.est.0c03558

Author Contributions

∥B.Z. and P.Y. contributed equally to this work.

Notes

The authors declare no competing financial interest.

■ ACKNOWLEDGMENTS

■ REFERENCES

(1) Flemming, H.- C.; Wingender, J. The biofilm matrix. *Nat. Rev. Microbiol.* **2010**, *8*, 623–633.

(2) Syron, E.; Casey, E. Membrane-aerated biofilms for high rate biotreatment: performance appraisal, engineering principles, scale-up, and development requirements. *Environ. Sci. Technol.* **2008**, *42*, 1833–1844.

(3) Price, J. E.; Chapman, M. R. Phaged and confused by biofilm matrix. *Nat. Microbiol.* **2018**, *3*, 2–3.

(4) De Smet, J.; Hendrix, H.; Blasdel, B. G.; Danis-Wlodarczyk, K.; Lavigne, R. *Pseudomonas* predators: understanding and exploiting phage–host interactions. *Nat. Rev. Microbiol.* **2017**, *15*, 517–530.

(5) Nadell, C. D.; Drescher, K.; Foster, K. R. Spatial structure, cooperation and competition in biofilms. *Nat. Rev. Microbiol.* **2016**, *14*, 589–600.

(6) Aw, T. G.; Rose, J. B. Detection of pathogens in water: from phylochips to qPCR to pyrosequencing. *Curr. Opin. Biotechnol.* **2012**, *23*, 422–430.

(7) Simmons, M.; Drescher, K.; Nadell, C. D.; Bucci, V. Phage mobility is a core determinant of phage-bacteria coexistence in biofilms. *ISME J.* **2018**, *12*, 531–543.

(8) Morris, C. E.; Monier, J.-M. The ecological significance of biofilm formation by plant-associated bacteria. *Annu. Rev. Physiol.* **2003**, *41*, 429–453.

(9) Díaz-Pascual, F.; Hartmann, R.; Lempp, M.; Vidakovic, L.; Song, B.; Jeckel, H.; Thormann, K. M.; Yildiz, F. H.; Dunkel, J.; Link, H.; Nadell, C. D.; Drescher, K. Breakdown of vibrio cholerae biofilm architecture induced by antibiotics disrupts community barrier function. *Nat. Microbiol.* **2019**, *4*, 2136–2145.

(10) Dion, M. B.; Oechslin, F.; Moineau, S. Phage diversity, genomics and phylogeny. *Nat. Rev. Microbiol.* **2020**, *18*, 125–138.

(11) Hansen, M. F.; Svenningsen, S. L.; Roder, H. L.; Middelboe, M.; Burmolle, M. Big impact of the tiny: bacteriophage-bacteria interactions in biofilms. *Trends Microbiol.* **2019**, *27*, 739–752.

(12) Dąbrowska, K. Phage therapy: what factors shape phage pharmacokinetics and bioavailability? systematic and critical review. *Med. Res. Rev.* **2019**, *39*, 2000–2025.

(13) Vidakovic, L.; Singh, P. K.; Hartmann, R.; Nadell, C. D.; Drescher, K. Dynamic biofilm architecture confers individual and collective mechanisms of viral protection. *Nat. Microbiol.* **2018**, *3*, 26–31.

(14) Bhattacharjee, A. S.; Choi, J.; Motlagh, A. M.; Mukherji, S. T.; Goel, R. Bacteriophage therapy for membrane biofouling in membrane bioreactors and antibiotic- resistant bacterial biofilm. *Biotechnol. Bioeng.* **2015**, *112*, 1644–1654.

(15) Townsley, L.; Shank, E. A. Natural-product antibiotics: cues for modulating bacterial biofilm formation. *Trends Microbiol.* **2017**, *25*, 1016–1026.

(16) Yu, P.; Mathieu, J.; Yang, Y.; Alvarez, P. J. J. Suppression of enteric bacteria by bacteriophages: importance of phage polyvalence in the presence of soil bacteria. *Environ. Sci. Technol.* **2017**, *51*, 5270–5278.

(17) Lu, T. K.; Collins, J. J. Dispersing biofilms with engineered enzymatic bacteriophage. *Proc. Natl. Acad. Sci. U.S.A.* **2007**, *104*, 11197–11202.

(18) Mathieu, J.; Yu, P.; Zuo, P.; Da Silva, M. L. B.; Alvarez, P. J. J. Going viral: emerging opportunities for phage-based bacterial control in water treatment and reuse. *Acc. Chem. Res.* **2019**, *52*, 849–857.

(19) Yu, P.; Wang, Z.; Marcos-Hernandez, M.; Zuo, P.; Zhang, D.; Powell, C.; Pan, A. Y.; Villagrán, D.; Wong, M. S.; Alvarez, P. J. J. Bottom-up biofilm eradication using bacteriophage-loaded magnetic nanocomposites: a computational and experimental study. *Environ. Sci. Nano* **2019**, *6*, 3539–3550.

(20) Eriksen, R. S.; Svenningsen, S. L.; Sneppen, K.; Mitarai, N. A growing microcolony can survive and support persistent propagation of virulent phages. *Proc. Natl. Acad. Sci. U.S.A.* **2018**, *115*, 337–342.

(21) Davies, J.; Spiegelman, G. B.; Yim, G. The world of subinhibitory antibiotic concentrations. *Curr. Opin. Microbiol.* **2006**, *9*, 445–453.

(22) Pezzoni, M.; Pizarro, R. A.; Costa, C. S. Exposure to low doses of UVA increases biofilm formation in *Pseudomonas aeruginosa*. *Biofouling* **2018**, *34*, 673–684.

(23) Calabrese, E. J.; Baldwin, L. A. Defining hormesis. *Hum. Exp. Toxicol.* **2002**, *21*, 91−97.

(24) Calabrese, E. J. Hormesis: Why It is Important to Toxicology and Toxicologists. *Environ. Toxicol. Chem.* **2008**, *27*, 1451−1474.

(25) Chaudhry, R. M.; Nelson, K. L.; Drewes, J. E. Mechanisms of pathogenic virus removal in a full-scale membrane bioreactor. *Environ. Sci. Technol.* **2015**, *49*, 2815−2822.

(26) Gerba, C. P.; Betancourt, W. Q. Viral aggregation: impact on virus behavior in the environment. *Environ. Sci. Technol.* **2017**, *51*, 7318−7325.

(27) Wigginton, K. R.; Kohn, T. Virus disinfection mechanisms: the role of virus composition, structure, and function. *Curr. Opin. Virol.* **2012**, *2*, 84−89.

(28) Motlagh, A. M.; Bhattacharjee, A. S.; Goel, R. Biofilm control with natural and genetically-modified phages. *World J. Microbiol. Biotechnol.* **2016**, *32*, No. 67.

(29) Ye, M.; Sun, M.; Huang, D.; Zhang, Z.; Zhang, H.; Zhang, S.; Hu, F.; Jiang, X.; Jiao, W. A review of bacteriophage therapy for pathogenic bacteria inactivation in the soil environment. *Environ. Int.* **2019**, *129*, 488−496.

(30) Perrin, C.; Briandet, R.; Jubelin, G.; Lejeune, P.; Berthelot, M. A.; Rodrigue, A.; Dorel, C. Nickel promotes biofilm formation by *Escherichia coli* K-12 strains that produce curli. *Appl. Environ. Microbiol.* **2009**, *75*, 1723−1733.

(31) Testa, S.; Berger, S.; Piccardi, P.; Oechslin, F.; Resch, G.; Mitri, S. Spatial structure affects phage efficacy in infecting dual-strain biofilms of *Pseudomonas aeruginosa. Commun Biol.* **2019**, *2*, No. 405.

(32) Yu, P.; Mathieu, J.; Li, M.; Dai, Z.; Alvarez, P. J. Isolation of polyvalent bacteriophages by sequential multiple-host approaches. *Appl. Environ. Microbiol.* **2016**, *82*, 808−815.

(33) Fernández, L.; Gonzalez, S.; Campelo, A. B.; Martinez, B.; Rodriguez, A.; Garcia, P. Low-level predation by lytic phage phiIPLA-RODI promotes biofilm formation and triggers the stringent response in *Staphylococcus aureus. Sci. Rep.* **2017**, *7*, No. 40965.

(34) Sobsey, M. D.; Yates, M. V.; Hsu, F.-C.; Lovelace, G.; Battigelli, D.; Margolin, A.; Pillai, S. D.; Nwachuku, N. Development and evaluation of methods to detect coliphages in large volumes of water. *Water Sci. Technol.* **2004**, *50*, 211−217.

(35) Jachlewski, S.; Jachlewski, W. D.; Linne, U.; Brasen, C.; Wingender, J.; Siebers, B. Isolation of extracellular polymeric substances from biofilms of the thermoacidophilic archaeon *Sulfolobus acidocaldarius. Front. Bioeng. Biotechnol.* **2015**, *3*, No. 123.

(36) Yang, Y.; Alvarez, P. J. J. Sublethal concentrations of silver nanoparticles stimulate biofilm development. *Environ. Sci. Technol. Lett.* **2015**, *2*, 221−226.

(37) Yang, G.; Lin, J.; Zeng, E. Y.; Zhuang, L. Extraction and characterization of stratified extracellular polymeric substances in *Geobacter* biofilms. *Bioresour. Technol.* **2019**, *276*, 119−126.

(38) Dubois, M.; Gilles, K. A.; Hamilton, J. K.; Rebers, P. A.; Smith, F. Colorimetric method for determination of sugars and related substances. *Anal. Chem.* **1956**, *28*, 350−356.

(39) Gendimenico, G. J.; Bouquin, P. L.; Tramfqsch, K. M. Diphenylamine-Colorimetric Method for DNA Assay: A Shortened Procedure by Incubating Samples at 50°C. *Anal. Biochem.* **1988**, *173*, 45−48.

(40) Rowan, B. A.; Oldenburg, D. J.; Bendich, A. J. A high-throughput method for detection of DNA in chloroplasts using flow cytometry. *Plant Methods* **2007**, *3*, No. 5.

(41) Gu, Y. Q.; Li, T. T.; Li, H. Q. Biofilm formation monitored by confocal laser scanning microscopy during startup of MBBR operated under different intermittent aeration modes. *Process Biochem.* **2018**, *74*, 132−140.

(42) Xue, Z.; Sendamangalam, V. R.; Gruden, C. L.; Seo, Y. Multiple roles of extracellular polymeric substances on resistance of biofilm and detached clusters. *Environ. Sci. Technol.* **2012**, *46*, 13212−13219.

(43) Rivera, L.; Lopez-Patino, M. A.; Milton, D. L.; Nieto, T. P.; Farto, R. Effective qPCR methodology to quantify the expression of virulence genes in *Aeromonas salmonicida* subsp. salmonicida. *J. Appl. Microbiol.* **2015**, *118*, 792−802.

(44) Basso, J. T. R.; Ankrah, N. Y. D.; Tuttle, M. J.; Grossman, A. S.; Sandaa, R.-A.; Buchan, A. Genetically similar temperate phages form coalitions with their shared host that lead to niche-specific fitness effects. *ISME J.* **2020**, *14*, 1688−1700.

(45) Samson, J. E.; Magadán, A. H.; Sabri, M.; Moineau, S. Revenge of the phages: defeating bacterial defences. *Nat. Rev. Microbiol.* **2013**, *11*, 675−687.

(46) Calabrese, E. J.; Baldwin, L. A. Hormesis: the dose-response revolution. *Annu. Rev. Pharmacol. Toxicol.* **2003**, *43*, 175−197.

(47) Davies, J.; Spiegelman, G. B.; Yim, G. The world of subinhibitory antibiotic concentrations. *Curr. Opin. Microbiol.* **2006**, *9*, 445−453.

(48) Calabrese, E. J.; Baldwin, L. A. Toxicology rethinks its central belief. *Nature* **2003**, *421*, 691−692.

(49) Calabrese, E. J.; Mattson, M. P. How does hormesis impact biology, toxicology, and medicine? *NPJ Aging Mech. Dis.* **2017**, *3*, No. 13.

(50) Calabrese, E. J. Overcompensation stimulation: a mechanism for hormetic effects. *Crit. Rev. Toxicol.* **2001**, *31*, 425−470.

(51) McDougald, D.; Rice, S. A.; Barraud, N.; Steinberg, P. D.; Kjelleberg, S. Should we stay or should we go: mechanisms and ecological consequences for biofilm dispersal. *Nat. Rev. Microbiol.* **2012**, *10*, 39−50.

(52) Sakuragi, Y.; Kolter, R. Quorum-sensing regulation of the biofilm matrix genes (*pel*) of *Pseudomonas aeruginosa. J. Bacteriol.* **2007**, *189*, 5383−5386.

(53) Nai, C.; Meyer, V. From axenic to mixed cultures: technological advances aaccelerating a paradigm shift in microbiology. *Trends Microbiol.* **2018**, *26*, 538−554.

(54) Seviour, T.; Derlon, N.; Dueholm, M. S.; Flemming, H. C.; Girbal-Neuhauser, E.; Horn, H.; Kjelleberg, S.; van Loosdrecht, M. C. M.; Lotti, T.; Malpei, M. F.; Nerenberg, R.; Neu, T. R.; Paul, E.; Yu, H.; Lin, Y. Extracellular polymeric substances of biofilms: suffering from an identity crisis. *Water Res.* **2019**, *151*, 1−7.

(55) Milho, C.; Silva, M. D.; Alves, D.; Oliveira, H.; Sousa, C.; Pastrana, L. M.; Azeredo, J.; Sillankorva, S. *Escherichia coli* and *Salmonella Enteritidis* dual-species biofilms: interspecies interactions and antibiofilm efficacy of phages. *Sci. Rep.* **2019**, *9*, No. 18183.

(56) Kay, M. K.; Erwin, T. C.; McLean, R. J.; Aron, G. M. Bacteriophage ecology in *Escherichia coli* and *Pseudomonas aeruginosa* mixed-biofilm communities. *Appl. Environ. Microbiol.* **2011**, *77*, 821−829.

(57) Rodrigues, D. F.; Elimelech, M. Toxic effects of single-walled carbon nanotubes in the development of *E. coli* biofilm. *Environ. Sci. Technol.* **2010**, *44*, 4583−4589.

(58) Gödeke, J.; Paul, K.; Lassak, J.; Thormann, K. M. Phage-induced lysis enhances biofilm formation in *Shewanella oneidensis MR-1. ISME J.* **2011**, *5*, 613−626.

(59) Koo, H.; Allan, R. N.; Howlin, R. P.; Stoodley, P.; Hall-Stoodley, L. Targeting microbial biofilms: current and prospective therapeutic strategies. *Nat. Rev. Microbiol.* **2017**, *15*, 740−755.

(60) Payne, R. J.; Jansen, V. A. Understanding bacteriophage therapy as a density-dependent kinetic process. *J. Theor. Biol.* **2001**, *208*, 37−48.